

# JGR Biogeosciences

## RESEARCH ARTICLE

10.1029/2021JG006659

### Key Points:

- PLUE could identify the drivers of vegetation change based on observations
- Seasonal patterns of leaf area index trends in these two conjunctural regions are different
- Land management is a driver of the vegetation change in the Sanjiang Plain

### Supporting Information:

Supporting Information may be found in the online version of this article.

### Correspondence to:

T. Chen,  
[txchen@nuist.edu.cn](mailto:txchen@nuist.edu.cn)

### Citation:








Chen, T., Dolman, H., Sun, Z., Zeng, N., Gao, H., Miao, L., et al. (2022). Land management explains the contrasting greening pattern across China-Russia border based on Paired Land Use Experiment approach. *Journal of Geophysical Research: Biogeosciences*, 127, e2021JG006659. <https://doi.org/10.1029/2021JG006659>

Received 7 OCT 2021  
Accepted 20 MAY 2022

### Author Contributions:

**Conceptualization:** Tiexi Chen, Han Dolman, Zhanli Sun, Ning Zeng  
**Data curation:** Shengjie Zhou  
**Investigation:** Chuanshuang Liang  
**Methodology:** Tiexi Chen, Lijuan Miao, Guojie Wang  
**Software:** Tiexi Chen, Haiyang Gao  
**Supervision:** Han Dolman, Ning Zeng  
**Validation:** Tiexi Chen  
**Visualization:** Tiexi Chen, Haiyang Gao, Xin Chen  
**Writing – original draft:** Tiexi Chen, Han Dolman, Zhanli Sun, Lijuan Miao, Xueqiong Wei, Chaofan Li, Qifei Han, Tingting Shi, Guojie Wang  
**Writing – review & editing:** Tiexi Chen, Han Dolman, Zhanli Sun, Ning Zeng, Lijuan Miao, Xueqiong Wei, Chaofan Li, Qifei Han, Tingting Shi, Guojie Wang

## Land Management Explains the Contrasting Greening Pattern Across China-Russia Border Based on Paired Land Use Experiment Approach

Tiexi Chen<sup>1,2</sup> , Han Dolman<sup>3,4</sup> , Zhanli Sun<sup>5</sup>, Ning Zeng<sup>6</sup> , Haiyang Gao<sup>7</sup> , Lijuan Miao<sup>1</sup>, Xueqiong Wei<sup>1</sup>, Chaofan Li<sup>1</sup>, Qifei Han<sup>1</sup> , Tingting Shi<sup>8</sup> , Guojie Wang<sup>1</sup> , Shengjie Zhou<sup>1</sup>, Chuanshuang Liang<sup>1</sup>, and Xin Chen<sup>1</sup>

<sup>1</sup>Collaborative Innovation Center on Forecast and Evaluation of Meteorological Disaster, School of Geographical Sciences, Nanjing University of Information Science and Technology, Nanjing, China, <sup>2</sup>School of Geographical Sciences, Qinghai Normal University, Xining, China, <sup>3</sup>NIOZ Royal Netherlands Institute for Sea Research, Texel, The Netherlands, <sup>4</sup>Department of Earth Sciences, Vrije Universiteit Amsterdam, Amsterdam, The Netherlands, <sup>5</sup>Leibniz Institute of Agricultural Development in Transition Economies, Halle, Germany, <sup>6</sup>Department of Atmospheric and Oceanic Science and Earth System Science Interdisciplinary Center, University of Maryland, College Park, MD, USA, <sup>7</sup>School of Atmospheric Physics, Nanjing University of Information Science and Technology, Nanjing, China, <sup>8</sup>School of Applied Meteorology, Nanjing University of Information Science and Technology, Nanjing, China

**Abstract** The greening of the Earth over the last decades is predominantly indicated by the enhancements of leaf area index (LAI). Quantifying the relative contribution of multiple determinants, especially changes in climate and in land management changes (LMC), remains an arduous challenge. To solve this problem, we develop a simple yet novel data-driven method, called the Paired Land Use Experiment (PLUE), for mesoscale analysis. Using PLUE, we analyze vegetation development of the Sanjiang Plain, a transboundary plain between China and Russia, with roughly homogeneous climate but with distinct land management practices across the border-intensified agricultural development on China side (CNSP) versus largely little-disturbed natural vegetation on Russia side (RUSP). Both CNSP and RUSP LAI show significant trends ( $p < 0.05$ ), with the annual variability reaching values of  $9.8 \times 10^{-3} \text{ yr}^{-1}$  and  $11.3 \times 10^{-3} \text{ yr}^{-1}$ , respectively. However, in CNSP, the LAI increase is concentrated in the middle of the year, especially in five 8-day periods from 26 June to 28 July. During this period, the LAI trend of CNSP is much higher than that of RUSP, at  $92.7 \times 10^{-3} \text{ yr}^{-1}$  ( $p < 0.01$ ) and  $43.8 \times 10^{-3} \text{ yr}^{-1}$  ( $p < 0.01$ ), respectively. Meanwhile, LAI decreased in CNSP at the beginning and end of the growing season. The results show that different LMC practices lead to notably different seasonal variability in vegetation changes. The PLUE method offers a new potential tool in driver identification of vegetation greenness change based on observations. We argue for the necessity of parameterizing these different LMC in Earth system models.

**Plain Language Summary** The greening of the world has been widely reported. However, quantifying the relative contribution of the drivers, including climate change and land management changes is still challenging. To overcome current limitations of modeling and observation based statistical analysis, a general “Paired Land Use Experiment (PLUE)” method and a benchmark case is presented. Mesoscale experimental areas could be found, such as the Sanjiang Plain on the China-Russian border with relatively uniform climate change and typical land management differences. The contribution of land management could be obtained by abstracting the natural variations which is purely driven by the climatic factors. Therefore, using the PLUE method, different land management explains contrasting greening pattern across Russia-China border. It suggests that this method could be applied on numerous mesoscale regions to stitch together a global scale picture.

## 1. Introduction

The greening of the Earth over the last few decades is predominantly determined by enhancements of leaf area index (LAI) (C. Chen et al., 2019; Forzieri et al., 2017; Olsson et al., 2005; Z. Zhu et al., 2016) mostly estimated by remote sensing data such as AVHRR (Advanced Very High Resolution Radiometer) (Pinzon & Tucker, 2014) and MODIS (Moderate Resolution Imaging Spectroradiometer) (Huete et al., 2002). Quantifying the response of vegetation to climate change and anthropogenic activity is crucial for understanding ecosystem dynamics per se,

for improving Earth system modeling (Bonan & Doney, 2018; Friedlingstein et al., 2014; Friend et al., 2014), and for future climate projections (Booth et al., 2012; Wenzel et al., 2014). Solar radiation, temperature, and water availability are the three classic climate constraints next to atmospheric CO<sub>2</sub> concentration that influence the global distribution of vegetation and its growth (Nemani et al., 2003).

Land cover change (LCC) and land management change (LMC), however, can also influence vegetation extent and functioning substantially through, for instance, deforestation, cropland expansion, multiple cropping, irrigation, and fertilizer use (T. Chen et al., 2022; Houghton, 2007; Huang et al., 2018; Z. Zhu et al., 2016). Quantifying the relative contribution of these different drivers to vegetation change has remained a difficult and arduous challenge (C. Chen et al., 2019; Z. Zhu et al., 2016). There are two categories of methods, including statistical analysis and Earth system models (ESMs), each with their own advantages and disadvantages. Statistical methods rely on correlation and coherent analyses and association physical process inference, with all their pitfalls, to infer something close to causality (Peng et al., 2013; X. Wang et al., 2011). Additionally, statistical models are analytical models—most of them are static in nature. ESMs are mostly process-based simulating models, and have the advantage that they can quantify the relative contribution of different factors and their interactions using sensitivity analysis approaches such as factorial experimental design (Le Quéré et al., 2009; Sitch et al., 2015). The premise here is that physical processes are fully understood and well described or parametrized (Huang et al., 2018; Mao et al., 2016; Z. Zhu et al., 2016). In general, climate factors and growing conditions are reasonably well captured and parameterized in ESMs. However, models with dynamics vegetation processes usually overestimate the contribution of CO<sub>2</sub> fertilizer effect (Huang et al., 2018; Mao et al., 2016; Z. Zhu et al., 2016), which is subject to several constraints that are currently poorly represented in models, such as nutrient limitation, land use change, and land managements (Fleischer et al., 2019; Jiang et al., 2019; Medlyn et al., 2015; Norby et al., 2010; Peñuelas et al., 2017; Reich et al., 2018; A. Smith et al., 2014; Walker et al., 2015). The potential impact of LMC, especially agricultural activities, is also not well incorporated in these models (Bonan & Doney, 2018; Erb et al., 2017; Levis et al., 2012; Pongratz et al., 2018). A good example is provided by the impact of the Agricultural Green Revolution, which is a classic agricultural intensification case where chemical fertilizers, synthetic pesticides, high-yield crop varieties, and multiple cropping were introduced in a system where the land cover (and land use) remains largely intact. In this paper, land management refers to the use and management of land resources, but excluding LCC (Erb et al., 2018; Houghton et al., 2012; Luyssaert et al., 2014). For instance, within a land cover type of cropland, land management includes fertilizer usage, irrigation, pesticides application, crop rotation and alteration, agricultural mechanization, and so on. Once the Agricultural Green Revolution was incorporated in a model, the stimulation of LAI and productivity helped to explain the observed increasing atmospheric CO<sub>2</sub> seasonal amplitude (Zeng et al., 2014). A recent study further emphasized the essential contribution of croplands to global greening and highlighted the requirement to improve the description of anthropogenic land use practices in models (C. Chen et al., 2019). However, there is still a lack of effective methods to identify the drivers and quantify the contributions from the regional to the global scale.

In this paper, we propose a novel method, called the “Paired Land Use Experiment (PLUE),” to disentangle the drivers of vegetation change, based on an approach similar to what hydrologist traditionally called “paired catchment analysis.” Rather than looking at the global scale to infer statistical relationships, or run a process-based simulation model, we take a region with a largely similar climate but with different land use practices (refers to both land management and land cover type) within the region, and then analyze the differences of vegetation development among the parts with distinct land use practices (Luyssaert et al., 2014). By conducting such a “natural experiment,” we can infer and quantify the effect of land use practices on the vegetation development as the climate factors are controlled. Because administrative boundaries often imply different land use policies, stimuli to economic development, and consequent land use practices on either side of the boundary, the task is to identify a large enough region with homogeneous climate that fulfills these criteria. The Sanjiang Plain, a trans-boundary plain along the border of China and Russia, is a perfect site for this kind of research. While intensified agriculture is prevalent on the China side, and the Russia part is large covered by natural vegetation. Using the PLUE approach, we analyze the interannual and seasonal changes of vegetation, estimate the contributions of climate change and LMC on both side of the border, and quantify the relative importance of climate and land management practices.

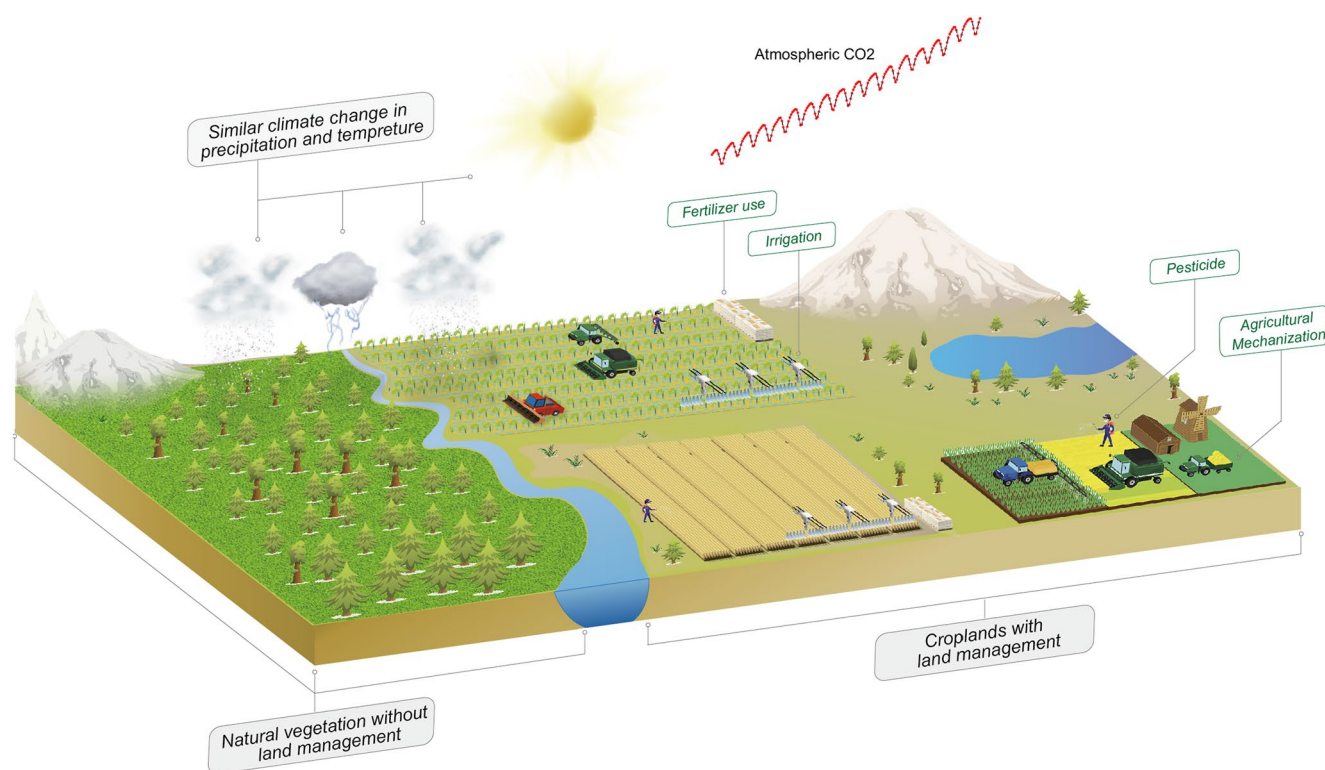


**Figure 1.** Schematic diagram of the Paired Land Use Experiment approach.

## 2. Materials and Methods

### 2.1. Paired Land Use Experiment Approach

The motivation of the PLUE proposed here is to identify the drivers of vegetation change based on observations. A recent study used this concept but has yet to provide a complete theoretical framework (T. Chen et al., 2022). The premise of PLUE is essentially based on the “natural experiment” approach: to infer and quantify the effects of a treatment while other independent variables are controlled based on a natural configuration. In the case of PLUE, we try to assess the effects of land management on the dynamics of LAI by controlling climate factors under a natural cross-border configuration. The general procedure of PLUE can be described as follows: select a region which is large enough but still with a roughly homogeneous climate environment. Two parts of such a region have different land use practices, and typical examples are natural vegetation and managed lands (such as croplands), or two managed lands with different intensity levels. At least one part has a stable land cover type. Therefore, these two regions could be treated as a PLUE with identical climate change forcing. The difference of vegetation response to environment could be contributed to land use change and land management change. Two objectives are expected: first, to identify the significance of the impact of human activities with natural control experiment of climate environment change. Second, to quantify the contributions of human activities by abstracting natural variations (a base line of the climatic influences). While, the premise required by the second goal is not easy to achieve in reality and is based on certain assumptions.

In particular, the area should not be too small, causing excessive interference, or not be too large, leading to inconsistent climate change within the region. A suggested scale is  $0.1\text{--}10 \times 10^4 \text{ km}^2$ , which is equivalent to a square area with a side length of 31.6–316 km. A schematic diagram is demonstrated in Figure 1.

### 2.2. The Sanjiang Plain

The Sanjiang Plain, which literally means three-river plain, is located in the plain area at the junction of Amur-Heilong River, Songhua River, and Ussuri River, covering a boundary region of China and Russia. This area includes parts of Heilongjiang Province of China and the Jewish Autonomous Oblast and the Khabarovsk Krai



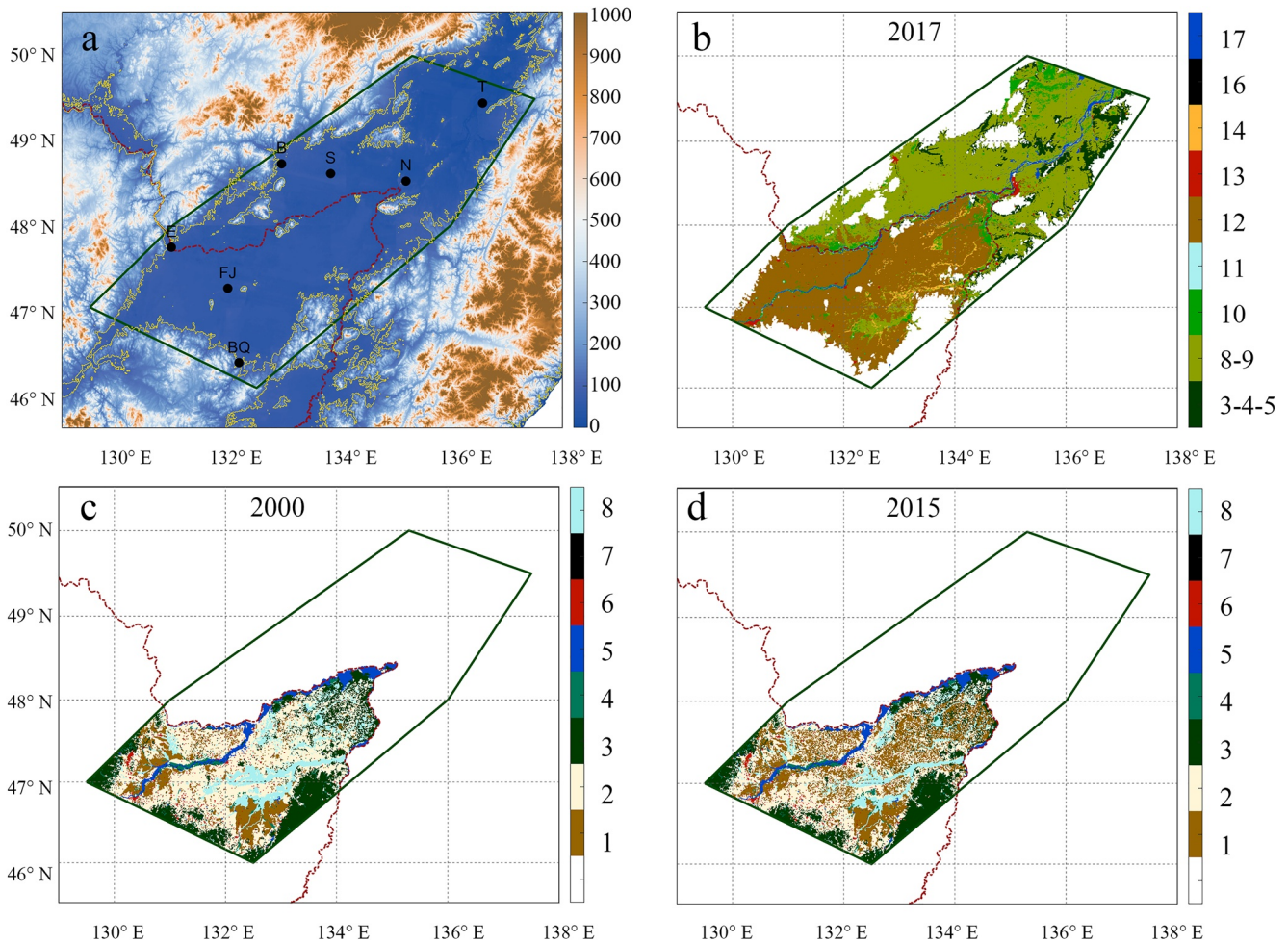


**Figure 2.** The location of Sanjiang Plain and its land cover types. (a) Location of the study plain and its topography. The 100 m height contour line is drawn in yellow. Meteorological sites in Russia and China are indicated by black dots with single-character or double-character labels, respectively (corresponding to Table S1 in Supporting Information S1). (b) Land cover of 2017 from MODIS land cover product (MCD12Q1, v006). Croplands (NO.12) are dark golden brown and savanna (NO.8–9) is sea green. Further detail of the International Geosphere-Biosphere Programme legend in Table 1. (c and d) Land cover type of 2 years of 2000 and 2015 based on RESDC data (Only data of China region are available in this data set). The land use types represented by serial numbers 1–8 are Paddy cropland, dry cropland, woodland, grassland, water body, build land, unused land, and wetlands. More detail of the legend is listed in Table 2.

of Russia. The Chinese and Russian parts of the Sanjiang Plain, splitting by the national boundary, are hereafter referred to as CNSP and RUSP, respectively. An irregular hexagon was drawn to outline the study area. The hexagon used to identify the approximate extent of the study area is located at these points of [47°N, 129.5°E], [46°N, 132.5°E], [48°N, 136°E], [49.5°N, 137.5°E], [50°N, 135.3°E], and [48°N, 131°E]. The topography is derived from Global 30 Arc-Second Elevation (GTOPO30) data set (<https://www.usgs.gov/>, <https://doi.org/10.5066/F7DF6PQS>). A height (above mean sea level) of 100 m was used as the threshold for extracting the plain with the small uplifts and hills and mountain edges were eliminated (Figure 2).

### 2.3. Precipitation and Temperature Records

Since observational meteorological data in this plain is difficult to attain, several other independent data sets were used. Three-hour temperature situ data from the Integrated Surface Dataset–Lite (ISD–Lite) (A. Smith et al., 2011) were obtained from the National Centers for Environmental Information (NCEI) for the Russian part of the plain. Although the data set also contains precipitation data, their reliability was deemed too poor for this region to be used. Five stations that cover the study period were chosen (Figure 2a, Table S1 in Supporting

**Table 1**  
*Land Cover Types Derived From Figures 2c, 2d and the Percentages of Each Type Using MODIS Land Cover Product*

Class	IGBP class name	CNSP 2001	CNSP 2017	Changes	RUSP 2001	RUSP 2017	Changes
3–4–5	Forest (3 Deciduous Needleleaf Forests, 4 Deciduous Broadleaf Forests, 5 Mixed Forests)	0.44	0.50	0.06	11.13	11.88	0.75
8–9	Savannas (8 Woody Savannas 9 Savannas)	5.60	8.06	2.46	76.40	74.89	−1.49
10	Grasslands	3.05	4.57	1.52	6.01	6.79	0.78
11	Permanent Wetlands	0.16	0.37	0.21	0.16	0.32	0.16
12	Croplands	85.54	80.67	−4.87	2.77	2.58	−0.19
13	Urban and Built-up Lands	0.69	0.71	0.02	0.73	0.73	0.00
14	Cropland/Natural Vegetation Mosaics	2.74	3.34	0.60	0.00	0.02	0.02
16	Barren	0.01	0.01	0.00	0.01	0.01	0.00
17	Water Bodies	1.77	1.77	0.00	2.79	2.79	0.00

*Note.* The changes are calculated as the percentages in 2017 subtract the percentages in 2001.

Information S1). For the Chinese part of the plain, we checked the data from China Meteorological Administration from (CMA). Only two sites can be used, that is, Fujin and Baoqing (Figure 2a, Table S1 in Supporting Information S1). Daily temperature and precipitation records during 2001–2017 from these seven stations were generated by averaging original 3-hr records at daily scales.

Gridded data sets were also used to compensate for the lack of site data. Monthly and 0.5° resolution Climatic Research Unit precipitation and temperature data (CRU TS4.02) (Harris et al., 2014), during 2001–2017 were obtained from the Centre for Environmental Data Analysis. In total, 26 and 34 grid points are included in Russian and Chinese parts of the plain (CNSP and RUSP), respectively.

In Table S1 of Supporting Information S1, the correlation between regional average CRU data and each site on annual and monthly scales is shown. The regional mean temperature and precipitation have a good correlation ( $p < 0.01$ ) with the station observation on the interannual and monthly scales. Therefore, grid data are very consistent with field observations.

## 2.4. Leaf Area Index

In this study, we use LAI to describe vegetation condition because LAI has a clear ecological meaning and is widely used in global greening studies. The 8-day 500 m resolution MODIS LAI (MOD15A2H, V006) (Myneni et al., 2015) were obtained from the LAADS DAAC (Level-1 and Atmosphere Archive & Distribution System Distributed Active Archive Center). Since the data are 8-day composites, in the following, the start date of each 8-day records is used as the time stamp.

## 2.5. Land Cover Type Products

The annual MODIS land cover product (MCD12Q1, v006) based on the International Geosphere-Biosphere Programme classification scheme (Friedl & Sulla-Menashe, 2015; Friedl et al., 2010) during 2001–2007 was used to delineate the vegetation cover spatial distribution (Table 1). This land cover data has the same spatial resolution (about 500 m) as the LAI data.

Cropland is one of the main types in MODIS land cover data, and there are no subcategories of cropland to differentiate various crop types. Therefore, another land use classification is also used here, provided by the Data Center for Resources and Environmental Sciences, Chinese Academy of Sciences (RESDC) at about 1 km resolution which were produced using Landsat TM/EM images (Liu et al., 2014). The data set contains six primary land use/land cover categories, including cropland, woodland, grassland, water body, settlements, and unused/barren land, these categories were further split into 25 subcategories. One of the outstanding features of this data

**Table 2**  
*Land Cover Types of Figure 2 and the Percentages of Each Component Using RESDC Product*

Class	RESDC class name	2000	2005	2010	2015	Changes	Change rate
0	Cropland	56.11	56.71	57.79	60.19	4.08	7.28
1	Paddy cropland	12.23	13.43	18.74	25.79	13.56	110.85
2	Dry cropland	43.87	43.28	39.05	34.40	−9.47	−21.59
3	Woodland	22.30	22.15	21.66	20.56	−1.74	−7.80
4	Grassland	2.55	2.73	2.67	2.56	0.01	0.50
5	Water body	5.40	5.42	5.45	5.43	0.03	0.51
6	Buildup land	1.84	1.84	1.82	1.83	−0.01	−0.50
7	Unused land	0.01	0.01	0.02	0.02	0.00	28.57
8	Wetlands	11.79	11.14	10.59	9.41	−2.38	−20.18

*Note.* The changes are calculated as the results of 2015 minus the results of 2000.

is the distinction between paddy fields and dry fields in the cropland. Previous studies have demonstrated that the land use change in the plain in the Chinese part is reflected in the conversion of wetlands to cropland, therefore, here we use 8 land use type groups: paddy cropland, dry cropland, woodland, grassland, water body, buildup land, and finally unused land wetlands. The RESDC data is not available at annual base, but is generated roughly every 5 years. Thus, during the study period, we used the data at 2000 and 2015.

Figure 2b shows the spatial distributions of land cover types based on MODIS data in the study area in 2017. The CNSP and RUSP regions have distinct land cover types, with the national border serving as the boundary. In China, cropland is the dominant land cover type, accounting for 85.54% in 2001% and 80.67% in 2017. In contrast, in Russia, natural vegetation, mainly forest and savannas, is dominant and cropland only takes into less than 3% of the area. Table 2 shows the proportions of major land cover types. In both CNSP and RUSP, the main land cover types show little change from 2001 to 2017.

## 2.6. Seasonal Pattern Variations

To show the evolution of seasonal characteristics over time, we divide the period of 2001–2017 roughly equally into three periods: 2001–2006, 2007–2012, and 2013–2017. Seasonal averages and deviations of these three periods and the whole study period were calculated.

## 2.7. Cumulative Correlation Matrix

In order to identify the time period when the interannual LAI is most sensitive to temperature and precipitation, we use a cumulative correlation matrix (CCM) method to exhaust all potential combinations. A multiyear time series (2001–2017) of temperature and precipitation for all consecutive months (including a single month) was calculated and then correlated with LAI. The correlation coefficients ( $r$ ) are presented in the form of a triangular matrix. The value in row  $i$  of column  $j$  ( $r_{i,j}$ ) denotes the correlation between annual averaged LAI and the temperature (or precipitation) averaged from month  $i$  to month  $j$ . For instance,  $r_{4,6}$  is the correlation between annual (January–December averaged) LAI and April–June averaged temperature (or precipitation), and  $r_{1,12}$  is the correlation between annual averaged LAI and annual averaged temperature (or precipitation).

## 2.8. Statistical Methods

The Pearson correlation coefficient was applied to quantify the relationship between two variables. The Mann-Kendall test is applied to determine the significance of the trends. A linear trend analysis on the LAI residuals was performed. The residuals of LAI were calculated by removing the multiple linear regression of the

climate factors (temperature and precipitation) from original annual averaged LAI time series. The determination coefficient ( $R^2$ ) and the  $F$ -test were applied to evaluate the linear regression and corresponding significances.

### 3. Results

In this section, the greening phenomenon in these two regions was first analyzed, which is followed by the diver identification from both climate change and land managements.

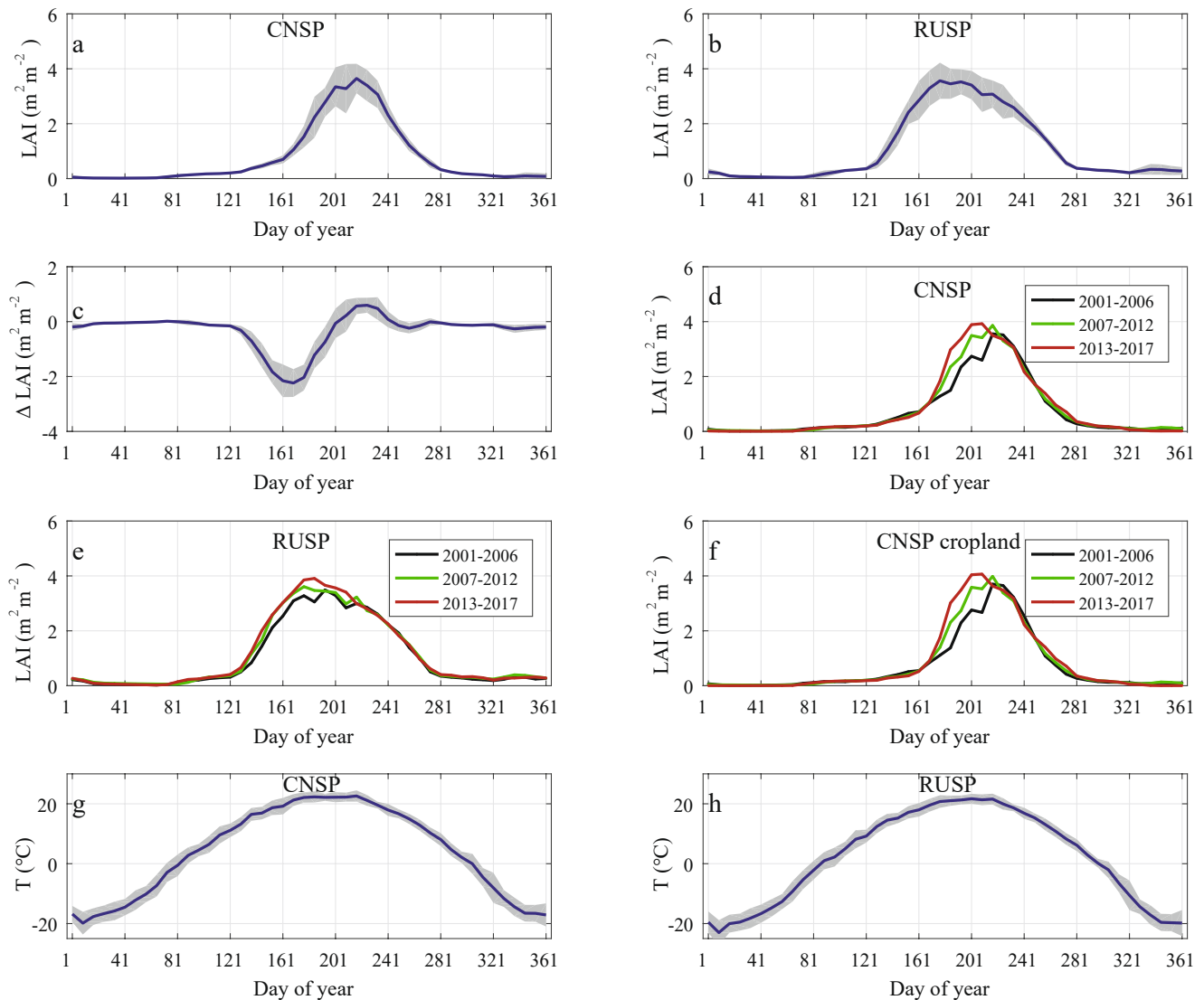
#### 3.1. Vegetation Development in the Sanjiang Plain

Figure 2b shows the spatial distributions of land cover types based on MODIS data in the study area in 2017 (see Section 2). The CNSP and RUSP regions have distinct land cover types, with the national border serving as the boundary. In China, cropland is the dominant land cover type, accounting for 85.54% in 2001% and 80.67% in 2017. In contrast, in Russia, natural vegetation, mainly forest and savannas, is dominant and cropland only takes into less than 3% of the area. Table 2 shows the proportions of major land cover types. In both CNSP and RUSP, the main land cover types show little change from 2001 to 2017.

The vegetation phenology characteristics of CNSP and RUSP are rather different. Data from the multiyear average seasonal characteristics (see Section 2) during 2001–2017 shows that the peak LAI in CNSP appears on 5 August (day 217), about 40 days later than that in RUSP, 26 June (day 177) (Figures 3a and 3b). The growing season in CNSP is shorter and relatively concentrated; the length of the periods with LAI greater than 1.0 and 2.0 are 96 and 64 days, respectively, in contrast to 136 and 96 days in RUSP. During the early growing season (day 121–201), the LAI in CNSP is also significantly lower than that in RUSP, showing the typical undulation, with the largest difference less than  $-2.0$  (Figure 3c). After 20 July (day 201) the LAI growth in CNSP became slightly higher than that in RUSP, with a difference of less than 1.0. Overall, the LAI fluctuates from relatively low to relatively high in CNSP in a short period, compared to a relatively stable LAI in RUSP.

To show the evolution of seasonal characteristics over time, we divide the period of 2001–2017 into three roughly equal length periods: 2001–2006, 2007–2012, and 2013–2017 (see Section 2). In CNSP, the LAI shows an overall one-way phase change during the three periods, and the LAI significantly increased particularly from 18th June to 5th August (day 169–217). During the period of 2013–2017, the seasonal peak appears 16 days earlier compared to the period of 2001–2006 (Figures 3d and 3e). The LAI growth is clearly concentrated in the first half time of the growing season. Further analysis of the cropland pixels (grid pixels identified as cropland from 2001 to 2017, accounting for 76.06% of the area) shows that the LAI seasonal variation in the three periods is very similar to the whole CNSP (Figure 3f). As natural vegetation is the predominant type in RUSP, the growing season is longer than that in CNSP. Compared with CNSP, the LAI increase in RUSP thus prolonging itself slightly longer during 2013–2017 than during 2001–2006.

Both CNSP and RUSP LAI show significant trends ( $p < 0.05$ ), with the annual variability of LAI reaching values of  $9.8 \times 10^{-3} \text{ yr}^{-1}$  and  $11.3 \times 10^{-3} \text{ yr}^{-1}$ , respectively (Figures 4a and 4b). The interannual variations in the two regions are similar ( $r = 0.805$ ,  $p < 0.01$ ) indicating that the interannual fluctuations of LAI in the two regions are driven by a similar climate and natural condition. This implies that our prime prerequisite for a PLUE is fulfilled. However, although the multiyear growth trends in CNSP and RUSP are similar, the seasonal patterns of LAI importantly show differences (Figure 4). In CNSP, the LAI increase is concentrated in the middle of the year, especially in five 8-day periods from the 26th June to 28th July (day 177–209). Among these, the multiyear mean variability of four 8-day periods exceeded  $50 \times 10^{-3}$  every year (Figure 4c), and the maximum value on the day 185 has a trend of  $122.8 \times 10^{-3} \text{ yr}^{-1}$  ( $p < 0.01$ ). The absolute value of the LAI decrease is still significantly less than that of the increase, thus the annual LAI overall exhibits an increasing trend. Most records (36 out of 48) in RUSP also showed a positive trend (Figure 4d). In CNSP, the seasonal characteristics of the LAI variability are very concentrated, especially during the five 8-day periods of 26 June to 28 July. During this period, the LAI trend of CNSP is much higher than that of RUSP, at  $92.7 \times 10^{-3} \text{ yr}^{-1}$  ( $p < 0.01$ ) and  $43.8 \times 10^{-3} \text{ yr}^{-1}$  ( $p < 0.01$ ), respectively. A similar situation occurs in the spatial patterns of LAI trends. As illustrated in Figure 5, although both CNSP and RUSP demonstrate a general greening pattern (Figure 5a) with identical amplitude, LAI trends in CNSP are overwhelmingly larger than that of RUSP during the period from the 26th June to 28th July (day 177–209). This suggests that the driving factors for intra-seasonal variations are different for CNSP and RUSP.



**Figure 3.** Seasonal patterns of leaf area index (LAI) and temperature. (a) and (b) Seasonal patterns of LAI during 2001–2017 over Chinese and Russian sides (CNSP and RUSP) of the Sanjiang plain. (c) The LAI difference by  $LAI_{CNSP} - LAI_{RUSP}$ . Blue curves are the averages of each month with standard deviations indicated by gray areas. (d and e) The annual average values from three difference periods of 2001–2006, 2007–2012, and 2013–2017. (f) The seasonal LAI of pure croplands. Pure cropland pixels are defined as grid points that are always identified as cropland in International Geosphere-Biosphere Programme during the study period, which account for about 76% area of the plain. (g and h) The seasonal cycles of temperature ( $T$ ) during 2001–2017 based on stations averaged records of the CNSP and RUSP parts.

### 3.2. Climate as a Potential Driver of Vegetation Change in the Sanjiang Plain

Based on the CRU gridded data (see Materials and methods), the annual averaged temperatures of CNSP and RUSP are 3.6 and 1.9°C, respectively, during 2001–2017. The multiyear average precipitation is 602 mm in CNSP and 676 mm in RUSP, most of the rainfall falls between May and September. The annual averaged temperatures in both regions show no significant increasing/decreasing trend and have no significant correlation with the LAI time series (Figures S1–S3 in Supporting Information S1). Wetting trends in CNSP and RUSP are found to be similar, 10.5 and 10.7 mm yr<sup>-1</sup>, respectively. However, no significant correlation is found between annual precipitation and LAI in these two regions. Therefore, we need to find the key climate periods that affect the annual changes of LAI, rather than using the annual averages of temperature and precipitation.

Cumulative correlation matrix of temperature and rainfall is shown in Figure S4 of Supporting Information S1 (see Materials and methods). Temperature in July has the greatest influence on the LAI interannual



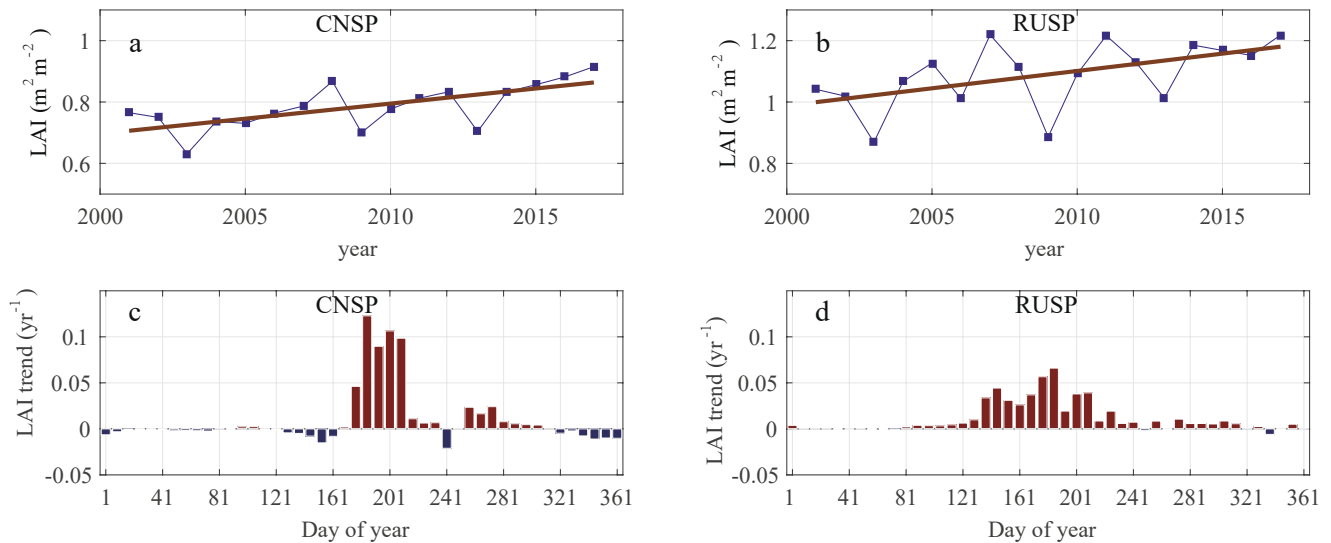


**Figure 4.** Trends of leaf area index (LAI) during 2001–2017. (a and b) Annual averaged time series and linear fits of LAI of CNSP and RUSP. (c and d) Linear trends in intra-seasonal LAI of each 8-day of CNSP and RUSP regions.

fluctuation ( $r = 0.74$ ,  $p < 0.01$ ) in CNSP. In RUSP, July temperature is also well correlated with annual averaged LAI ( $r = 0.65$ ,  $p < 0.01$ ), but the maximum correlation is found to be with the average temperature of whole July–September period ( $r = 0.73$ ,  $p < 0.01$ ). The total precipitation in May–June is positively correlated with LAI ( $r = 0.65$ ,  $p < 0.01$ ) in CNSP. In RUSP, the maximum positive correlation corresponds to the total precipitation in April–May ( $r = 0.47$ ,  $p = 0.058$ ), start of the growing season. This suggests that precipitation is important at the start of the growing season for both CNSP and RUSP. The time difference of precipitation here (May–June and April–May) is related to the phenological difference between the two places (Figures 3a and 3b).

Since both temperature and precipitation have key periods that correlated with annual averaged LAI mostly, a multiple linear regression using temperature and precipitation as the two explanatory variables was applied. Temperature in July and precipitation in May–June could well fit LAI over the CNSP region ( $R^2 = 0.74$ ,  $p < 0.01$ ) (Figure S5 in Supporting Information S1). The trend of the residual is only about  $0.9 \times 10^{-3} \text{ yr}^{-1}$  ( $p = 0.64$ , not significant), which is less than one-tenth of the original LAI trend (Figure 4). A similar analysis for the RUSP region using temperature in July–September and its combination with precipitation in April–May gives values

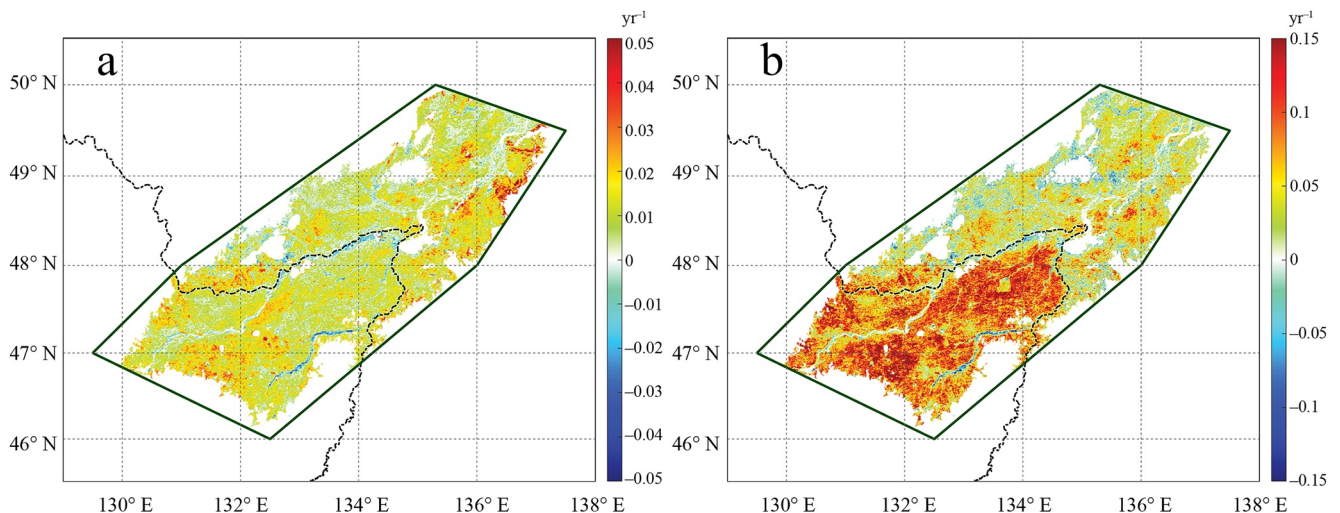


**Figure 5.** Grid trends of leaf area index (LAI, m<sup>2</sup> m<sup>-2</sup> yr<sup>-1</sup>). (a) The spatial patterns of LAI trends during 2001–2017 based on the annual averaged time series. (b) The spatial patterns of LAI trends during 2001–2017 based on the averaged time series of the period from the 26th June to 28th July (day 177–209).

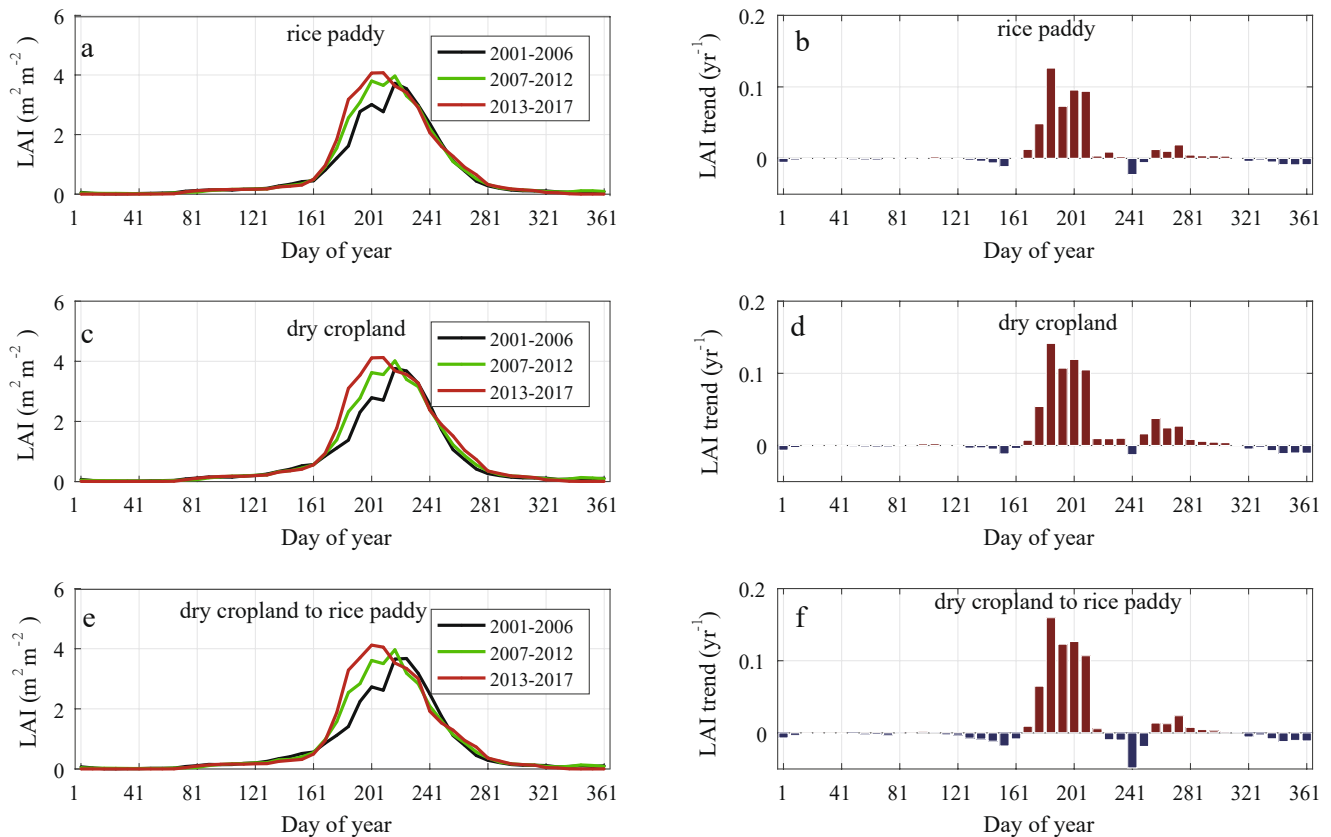


**Figure 6.** Seasonal patterns of multi-annual average and linear trends of leaf area index over China croplands. (a and b) Pure rice paddy lands. (c and d) Pure dry cropland. (e and f) The area changing from dry cropland to rice paddy.

of  $R^2 = 0.54$ ,  $p < 0.01$  (Figure S5 in Supporting Information S1). The trend of the residuals is  $2.9 \times 10^{-3} \text{ yr}^{-1}$ , about a quarter of the trend (Figure 4). Although it thus appears that climatic constraints can explain the interannual variations and trends of LAI, behind the differences in seasonal variability of the CNSP and RUSP regions (Figure 4), including concentrated increasing periods and some decreasing periods, lies likely another cause (Figure S1–S3 in Supporting Information S1). Therefore, next we explore the changes in land use and particularly land management.

### 3.3. Land Management as a Driver of the Vegetation Change in the Sanjiang Plain

Obviously, the life cycle of cropland vegetation in the CNSP region is very different from that of natural vegetation in RUSP. First, the life cycle of cropland vegetation, from germination to harvest, is much shorter. In particular, the beginning of the growing period is entirely dependent on the time of sowing (although small-scale variability in weather may also affect the agricultural schedule to a minor extent).

To further explain the seasonal characteristics of LAI trends in CNSP, we explore the changes of types of crop variety in cropland, the development of agricultural science and technology as possible causes. As can be seen from Table 2 and Figure 6, the most significant change of land management in this area is the rice paddy expansion. Rice plantation area has doubled from 2000 to 2015, rising from 12.2% to 25.8%. Most new paddy fields are converted from dry cropland, and the decrease of dry cropland accounts for 9.5% of the total area. At the same time, the proportions of wetland and woodland decrease by only 2.4% and 1.7%, respectively. Land management change within agriculture is clearly the major change in this area.

The multi-year trends of the key cropland types, rice paddy, dry cropland, and rice paddy converted from dry cropland, show similar patterns (Figure 5), with all three land use types showing a significant LAI increase in the first half of the growth stage. At the same time, the average LAI growth rate in the converted land from 26 June

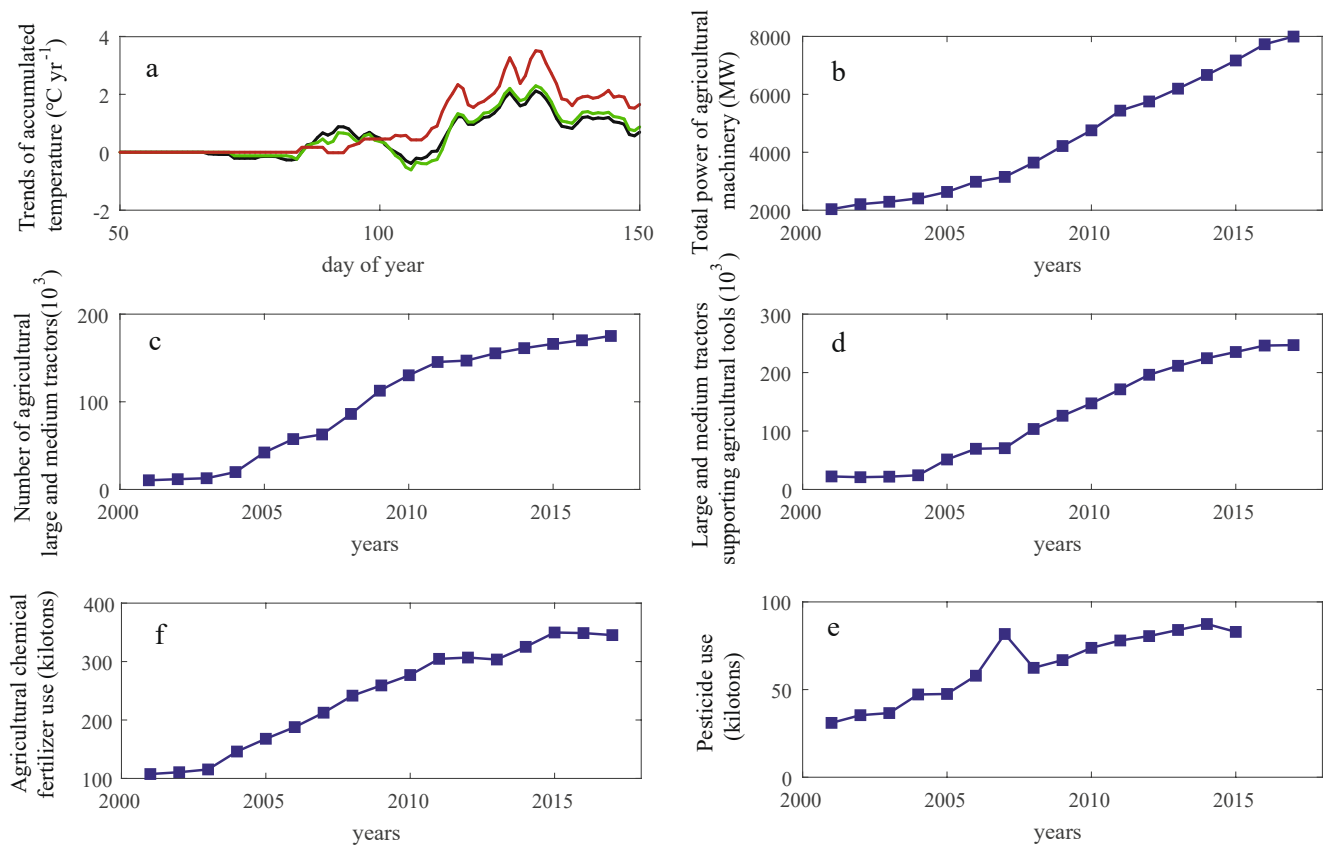


**Figure 7.** Factors impacting agricultural management of CNSP. (a) Trends of accumulated temperature on days with a mean daily temperature above 0°C (black), 5°C (green), and 10°C (red) during 2001–2017, day 50, 100, and 150 of year are corresponding to 26th February, 17th April, and 6th June. (b) Total power of agricultural machinery. (c) The number of agricultural large and medium tractors. (d) Large and medium tractors supporting agricultural tools. (e) The usage of agricultural chemical fertilizer. (f) The usage of pesticide (province level).

to 28 July is higher than that for pure paddy fields or dry cropland. It is noteworthy that during the period of 9 May–10 June, especially on 29 August, there is a strong decreasing trend for the converted land. This change is mainly caused by the expansion of paddy fields and the wider range of flooding during the transplanting period, while in the late growing season, paddy fields turn yellow earlier than other dry croplands (e.g., maize).

The Heilongjiang Province experienced rapid mechanization of agriculture during the study period. The data provided by the National Bureau of Statistics and Heilongjiang Bureau of Statistics at provincial and prefecture-level city level provides evidence for the mechanization development of CNSP. CNSP involves three cities: Jiamusi, Hegang, and Shuangyashan. Only the pesticide usage is at the provincial level, and the rest of the data are the average of the three cities. As shown in Figure 7, the total power of agricultural machinery increased from 2,035 to 7,995 MW, or an increase of 292.87%, during 2001–2017; the number of large and medium-sized agricultural tractors increased from 10,468 to 175,070, or an increase of 1572.43%; the number of matching agricultural tools of large and medium-sized tractors increased from 22,259 to 246,976, or an increase of 1009.55%; the effective amount of agricultural chemical fertilizer increased from 107.52 to 345.26 kilotons, or an increase of 221.11%; the use of pesticides of Heilongjiang province increased from 31.0 to 82.9 kilotons (until 2015), or an increase of 167.42%.

Overall, the use of fertilizers and pesticides in cropland has increased substantially, while the amount of agricultural machinery has increased by a factor larger than 10, implying that the time length of sowing should have been greatly shortened. At the same time, the area is at relatively high latitude so the length and the start of cropping season are, therefore, important factors influencing the crop growth. To illustrate this, we calculate the day numbers with mean daily temperatures above 0, 5, and 10°C to obtain the accumulated temperature (see Section 2). With an increase of accumulated temperature in spring (Figure 6a), farmers can sow earlier. Together

with the advancement of sowing and the shortening of planting period brought about by agricultural mechanization this moves the seeding stage to earlier dates.

Therefore, in summary, land managements could explain the differences in seasonal variability of the CNSP and RUSP regions. In particular, there are two main types of land management here. One is the transformation from dry land to paddy field within the scope of croplands, which is the main driver of the decreasing trends of LAI at the beginning and end of the growing season (Figure 6). The other is the agriculture modernization, including mechanization and the usage of fertilizers and pesticides, which resulted in the very concentrated increasing trends of LAI during the main growing periods of plants.

#### 4. Discussion

About 70% of the current global greening can be explained by CO<sub>2</sub> fertilization effect, which was suggested by previous studies (Z. Zhu et al., 2016). A recent research (C. Chen et al., 2019) noted that the greening is mostly prominent in croplands and advocated the need for improving the realistic description of human land use practices in models. However, they only inferred an indirect link between land management and vegetation change without solid driver identification and further quantifying the contribution. The study presented here provides a new perspective to disentangle the drivers by applying PLUE approach on a transboundary region, that is, the Sanjiang Plain along the China-Russia border. The premise is that a transboundary region with uniform terrain and climate but with distinct land management practices may offer the possibility to assess the relative contributions of climate change and land management change. Based on the above analysis of the results, we can further describe the hypothesis of the PLUE method in this case study specifically. The differences mainly include the very concentrated increasing periods and some decreasing periods in CNSP, which also demonstrate the typicality of the Sanjiang Plain case. If it is assumed that RUSP, with no major LMC in the last decades, shows a change that is driven by climatic and environmental factors, then the difference with CNSP must have been caused by land cover and land management change. Because there is little LCC (Table 2), this difference is then very likely to be caused by land management.

As demonstrated in the results section, similar significant increasing trends in annual LAI time series were found in both CNSP and RUSP at  $9.8 \times 10^{-3} \text{ yr}^{-1}$  ( $p < 0.05$ ) and  $11.3 \times 10^{-3} \text{ yr}^{-1}$  ( $p < 0.05$ ), respectively (Figures 4a and 4b). Using precipitation and air temperature, the LAI time series of both regions can be well fitted (Figure S5 in Supporting Information S1). However, the large differences in timing and trends in mainly phenology (the main crop growth period during the summer), between the two parts of the Sanjiang plain cannot be explained by climate differences. During the five 8-day periods of 26th June to 28th July period, the LAI trend of CNSP is much higher than that of RUSP, at  $92.7 \times 10^{-3} \text{ yr}^{-1}$  ( $p < 0.01$ ) and  $43.8 \times 10^{-3} \text{ yr}^{-1}$  ( $p < 0.01$ ), respectively. Therefore, residual analysis using annual average time series will give wrong results and be misleading.

The LAI changes of the RUSP part are predominantly caused by natural variability, implying that the observed doubling of the greening in the growing season and decline in the shoulder seasons in CNSP must be caused by LMC. Several important indicators of agricultural mechanization development in CNSP have doubled or even tripled during our period of study. As described above about the basic concept of the PLUE method, the contribution of land management could be obtained by abstracting the natural variations which is purely driven by the climatic factors. However, such a “base line” is not directly measurable. A rough but feasible way is finding a reference as the estimation of the “base line.” Therefore, naturally an assumption is made here using the change of natural vegetation of the RUSP region as an estimate. During the five 8-day periods of 26 June–28 July period, the “base line” is  $43.8 \times 10^{-3} \text{ yr}^{-1}$  in RUSP, while the combined natural and land management drive result is  $92.7 \times 10^{-3} \text{ yr}^{-1}$  in CNSP. This suggests that the impact of cropland management (not LCC) on the greening in this area is at similar magnitude as the impact of climate change. The potential error is also obvious, that is whether the response amplitudes of crops and natural vegetation to climate environment are the same. The higher (lower) estimate of the latter means a lower (higher) deduction on the impact of land management. Due to the differences in the geographical location (such as latitude) of the adjacent areas, the average precipitation and temperature of the two cannot be strictly the same, which could have a certain impact on the “control climate conditions.” In the Sanjiang Plain, CNSP is a little bit warmer (about 1.7°C) than RUSP as it is located on the south side of RUSP. From the perspective of the spatial pattern of vegetation change, because the national border



is very tortuous, the difference in vegetation change still takes the national border as a typical dividing line. The same latitude areas along the border still maintain the contrast difference (Figure 5).

Importantly, the LAI of CNSP also showed declining trends in some periods, compared to the RUSP region. Particularly during day 129–161, these five 8-day periods, LAI of CNSP exhibited an average decreasing rate at  $-8.1 \times 10^{-3} \text{ yr}^{-1}$ ; during the same period, the rate of LAI of the RUSP was  $29 \times 10^{-3} \text{ yr}^{-1}$ . This period corresponds to 9 May to 10 June, usually the first month after sowing. This decrease cannot be attributed to changes in climate. During 2000–2015, the CNSP region has experienced a rapid and massive rice paddy expansion which was mainly converted from dry croplands due to the economic purposes. For the rice paddy, during the transplanting period when the small seedlings are moved to a new field, the paddy fields need to be submerged, and the vegetation index is reduced due to the abundant water, which in turn affects the LAI value (Figure 6f).

As mentioned in the introduction, here we proposed a new approach in statistical methods rather than model simulation. This paper seeks to address the dilemma encountered by current statistical methods. As summarized by Piao et al. (2020), it is challenging to quantify the greening drivers individually. One of the most common attribution analyses is the residual analysis method that is still widely used today with hundreds of studies. Some recent studies have begun to use machine learning methods in residual analysis, such as using random forests instead of general regression fitting (Wu et al., 2020). However, it still cannot solve the inherent problem brought by its assumption that the effects of different drivers are linearly independent. A recent study applied the Geodetector (J. F. Wang et al., 2010) in greening driver identification based on spatially stratified heterogeneity analysis (L. Zhu et al., 2020). The Geodetector is widely used in geographical spatial pattern analysis, and whether it is suitable for this topic remains unclear because the Geodetector can only identify spatial-related elements, not driving factors.

The difficulties of current statistical methods are also reflected in the work revealed by C. Chen et al. (2019), which found a global greening phenomenon led by croplands, but did not clearly identify the driving factors. Our proposed method, including theory and typical case studies, demonstrates its effectiveness. However, how many regions around the world are capable for this theory, and how large the total extension will be, are both unclear yet. In contrast to “natural experiment,” how to conduct controlled experiments at the regional scale and the content design also need to be further explored. Land management contains very complex content, and natural experiments can only be inferred in general, and it also makes it difficult to combine control experiments with real situations.

## 5. Conclusion

Current land surface components in ESMs still only marginally consider land management (Erb et al., 2017; Pongratz et al., 2018; Zeng et al., 2014). Meanwhile, the question on driver identification raised by global widely distributed cropland greening (C. Chen et al., 2019) is still far from being solved due to the lack of effective study methods. The PLUE method initially proposed in this paper shows a way forward in identifying the LMC as drivers and quantifying these impacts. It is well-known, from for instance forestry and agricultural inventories, that boundaries in carbon content change suddenly as a result of land management when borders or geographical units are crossed. Our analysis shows how to make creative use of these differences to identify and quantify the impacts of land use management on vegetation change. Cross-border regions that fulfill PLUE criteria are theoretically widely distributed around the world because land management usually has typical political zoning characteristics. A typical case over the Sanjiang Plain, a transboundary plain along the border of China and Russia, demonstrated the application of the PLUE method and LMC is identified as an important factor affecting greening over the CNSP region. More cases are needed to make the PLUE method a sophisticated tool. Pursuing further studies in this issue may help to improve our understanding of the links between LMC and climate and develop new parametrizations for ESMs.

## Data Availability Statement

All data used in this article are available from open accessed scientific data resources. Land cover data (MOD12C1, V006) and LAI data (MOD15A2H, V006) are available at the LAADS DAAC (Level-1 and Atmosphere Archive & Distribution System Distributed Active Archive Center <https://ladsweb.modaps.eosdis.nasa.gov>). Global 30

Arc-Second Elevation (GTOPO30) are available at the U.S. Geological Survey (<https://www.usgs.gov/>, <https://doi.org/10.5066/F7DF6PQS>). Land cover data for CNSP are available at the Data Center for Resources and Environmental Sciences, Chinese Academy of Sciences (RESDC) (<http://www.resdc.cn>). CRU TS4.02 data are available at the Centre for Environmental Data Analysis (<http://browse.ceda.ac.uk/>). Meteorological site records are available at the National Centers for Environmental Information (NCEI, <https://www.ncei.noaa.gov/products/land-based-station/integrated-surface-database>) and CMA (<http://data.cma.cn/>). The post-processed results data corresponding to the plots/tables are available from the authors upon request ([txchen@nuist.edu.cn](mailto:txchen@nuist.edu.cn)).

## Acknowledgments

This research is supported by the National Natural Science Foundation of China (No. 42161144003, 42130506, and 31570464), the National Key R&D Program of China (No. 2017YFB0504000), A.J. Dolman acknowledges support from the program of the Netherlands Earth System Science Centre, financially supported by the Ministry of Education, Culture and Science (OCW) (Grant 024.002.001).

## References

- Bonan, G. B., & Doney, S. C. (2018). Climate, ecosystems, and planetary futures: The challenge to predict life in Earth system models. *Science*, 359(6375), eaam8328. <https://doi.org/10.1126/SCIENCE.AAM8328>
- Booth, B. B. B., Jones, C. D., Collins, M., Totterdell, I. J., Cox, P. M., Sitch, S., et al. (2012). High sensitivity of future global warming to land carbon cycle processes. *Environmental Research Letters*, 7(2), 024002. <https://doi.org/10.1088/1748-9326/7/2/024002>
- Chen, C., Park, T., Wang, X., Piao, S., Xu, B., Chaturvedi, R. K., et al. (2019). China and India lead in greening of the world through land-use management. *Nature Sustainability*, 2(2), 122–129. <https://doi.org/10.1038/s41893-019-0220-7>
- Chen, T., Guo, R., Yan, Q., Chen, X., Zhou, S., Liang, C., et al. (2022). Land management contributes significantly to observed vegetation browning in Syria during 2001–2018. *Biogeosciences*, 19(5), 1515–1525. <https://doi.org/10.5194/bg-19-1515-2022>
- Erb, K.-H., Kastner, T., Plutzer, C., Bais, A. L. S., Carvalhais, N., Fetzel, T., et al. (2018). Unexpectedly large impact of forest management and grazing on global vegetation biomass. *Nature*, 553(7686), 73–76. <https://doi.org/10.1038/NATURE25138>
- Erb, K.-H., Luyssaert, S., Meyfroidt, P., Pongratz, J., Don, A., Kloster, S., et al. (2017). Land management: Data availability and process understanding for global change studies. *Global Change Biology*, 23(2), 512–533. <https://doi.org/10.1111/GCB.13443>
- Fleischer, K., Rammig, A., Kauwe, M. G. D., Walker, A. P., Domingues, T. F., Fuchslueger, L., et al. (2019). Amazon forest response to CO<sub>2</sub> fertilization dependent on plant phosphorus acquisition. *Nature Geoscience*, 12(9), 736–741. <https://doi.org/10.1038/S41561-019-0404-9>
- Forzieri, G., Alkama, R., Miralles, D. G., & Cescatti, A. (2017). Satellites reveal contrasting responses of regional climate to the widespread greening of Earth. *Science*, 356(6343), 1180–1184. <https://doi.org/10.1126/SCIENCE.AAL1727>
- Friedl, M. A., & Sulla-Menashe, D. (2015). MCD12Q1 MODIS/Terra+qua land cover type yearly L3 global 500 m SIN grid V006 [Data set]. NASA EOSDIS Land Processes DAAC. <https://doi.org/10.5067/MODIS/MCD12Q1.006>
- Friedl, M. A., Sulla-Menashe, D., Tan, B., Schneider, A., Ramankutty, N., Sibley, A., & Huang, X. (2010). MODIS Collection 5 global land cover: Algorithm refinements and characterization of new datasets. *Remote Sensing of Environment*, 114(1), 168–182. <https://doi.org/10.1016/J.RSE.2009.08.016>
- Friedlingstein, P., Meinshausen, M., Arora, V. K., Jones, C. D., Anav, A., Liddicoat, S. K., & Knutti, R. (2014). Uncertainties in CMIP5 climate projections due to carbon cycle feedbacks. *Journal of Climate*, 27(2), 511–526. <https://doi.org/10.1175/JCLI-D-12-00579.1>
- Friend, A. D., Lucht, W., Rademacher, T. T., Kerbin, R., Betts, R., Cadule, P., et al. (2014). Carbon residence time dominates uncertainty in terrestrial vegetation responses to future climate and atmospheric CO<sub>2</sub>. *Proceedings of the National Academy of Sciences of the United States of America*, 111(9), 3280–3285. <https://doi.org/10.1073/PNAS.1222477110>
- Harris, I., Jones, P., Osborn, T., & Lister, D. (2014). Updated high-resolution grids of monthly climatic observations – The CRU TS3.10 Dataset. *International Journal of Climatology*, 34(3), 623–642. <https://doi.org/10.1002/JOC.3711>
- Houghton, R. A. (2007). Balancing the global carbon budget. *Annual Review of Earth and Planetary Sciences*, 35(1), 313–347. <https://doi.org/10.1146/ANNUREV.EARTH.35.031306.140057>
- Houghton, R. A., House, J. I., Pongratz, J., Van der Werf, G. R., DeFries, R. S., Hansen, M. C., et al. (2012). Carbon emissions from land use and land-cover change. *Biogeosciences*, 9(12), 5125–5142. <https://doi.org/10.5194/BG-9-5125-2012>
- Huang, K., Xia, J., Wang, Y., Ahlström, A., Chen, J., Cook, R. B., et al. (2018). Enhanced peak growth of global vegetation and its key mechanisms. *Nature Ecology and Evolution*, 2(12), 1897–1905. <https://doi.org/10.1038/S41559-018-0714-0>
- Huete, A., Didan, K., Miura, T., Rodriguez, E. P., Gao, X. Y., & Ferreira, L. G. (2002). Overview of the radiometric and biophysical performance of the MODIS vegetation indices. *Remote Sensing of Environment*, 83(1), 195–213. [https://doi.org/10.1016/S0034-4257\(02\)00096-2](https://doi.org/10.1016/S0034-4257(02)00096-2)
- Jiang, M., Caldararu, S., Zaehle, S., Ellsworth, D. S., & Medlyn, B. E. (2019). Towards a more physiological representation of vegetation phosphorus processes in land surface models. *New Phytologist*, 222(3), 1223–1229. <https://doi.org/10.1111/NPH.15688>
- Le Quéré, C. L., Raupach, M. R., Canadell, J. G., Marland, G., Bopp, L., Ciais, P., et al. (2009). Trends in the sources and sinks of carbon dioxide. *Nature Geoscience*, 2(12), 831–836. <https://doi.org/10.1038/NNGEO689>
- Levis, S., Bonan, G. B., Kluzek, E., Thornton, P. E., Jones, A., Sacks, W. J., & Kucharik, C. J. (2012). Interactive crop management in the Community Earth System Model (CESM1): Seasonal influences on land–atmosphere fluxes. *Journal of Climate*, 25(14), 4839–4859. <https://doi.org/10.1175/JCLI-D-11-00446.1>
- Liu, J., Kuang, W., Zhang, Z., Xu, X., Qin, Y., Ning, J., et al. (2014). Spatiotemporal characteristics, patterns, and causes of land-use changes in China since the late 1980s. *Journal of Geographical Sciences*, 24(2), 195–210. <https://doi.org/10.1007/S11442-014-1082-6>
- Luyssaert, S., Jammot, M., Stoy, P. C., Estel, S., Pongratz, J., Ceschia, E., et al. (2014). Land management and land-cover change have impacts of similar magnitude on surface temperature. *Nature Climate Change*, 4(5), 389–393. <https://doi.org/10.1038/NCLIMATE2196>
- Mao, J., Ribes, A., Yan, B., Shi, X., Thornton, P. E., Séférian, R., et al. (2016). Human-induced greening of the northern extratropical land surface. *Nature Climate Change*, 6(10), 959–963. <https://doi.org/10.1038/NCLIMATE3056>
- Medlyn, B. E., Zaehle, S., Kauwe, M. G. D., Walker, A. P., Dietze, M. C., Hanson, P. J., et al. (2015). Using ecosystem experiments to improve vegetation models. *Nature Climate Change*, 5(6), 528–534. <https://doi.org/10.1038/NCLIMATE2621>
- Myneni, R., Knyazikhin, Y., & Park, T. (2015). MOD15A2H MODIS/Terra leaf area index/FPAR 8-day L4 global 500 m SIN grid V006 [Data set]. NASA EOSDIS Land Processes DAAC.
- Nemani, R. R., Keeling, C. D., Hashimoto, H., Jolly, W. M., Piper, S. C., Tucker, C. J., et al. (2003). Climate-driven increases in global terrestrial net primary production from 1982 to 1999. *Science*, 300(5625), 1560–1563. <https://doi.org/10.1126/SCIENCE.1082750>
- Norby, R. J., Warren, J. M., Iversen, C. M., Medlyn, B. E., & McMurtrie, R. E. (2010). CO<sub>2</sub> enhancement of forest productivity constrained by limited nitrogen availability. *Proceedings of the National Academy of Sciences of the United States of America*, 107(45), 19368–19373. <https://doi.org/10.1073/PNAS.1006463107>

- Olsson, L., Eklundh, L., & Ardö, J. (2005). A recent greening of the Sahel—Trends, patterns and potential causes. *Journal of Arid Environments*, 63(3), 556–566. <https://doi.org/10.1016/J.JARIDENV.2005.03.008>
- Peng, S., Piao, S., Ciais, P., Myneni, R. B., Chen, A., Chevallier, F., et al. (2013). Asymmetric effects of daytime and night-time warming on Northern Hemisphere vegetation. *Nature*, 501(7465), 88–92. <https://doi.org/10.1038/NATURE12434>
- Peñuelas, J., Ciais, P., Canadell, J. G., Janssens, I. A., Fernández-Martínez, M., Carnicer, J., et al. (2017). Shifting from a fertilization-dominated to a warming-dominated period. *Nature Ecology and Evolution*, 1(10), 1438–1445. <https://doi.org/10.1038/S41559-017-0274-8>
- Piao, S., Wang, X., Park, T., Chen, C., Lian, X. U., He, Y., et al. (2020). Characteristics, drivers and feedbacks of global greening. *Nature Reviews Earth & Environment*, 1(1), 14–27. <https://doi.org/10.1038/s43017-019-0001-x>
- Pinzon, J. E., & Tucker, C. J. (2014). A non-stationary 1981–2012 AVHRR NDVI 3g time series. *Remote Sensing*, 6(8), 6929–6960. <https://doi.org/10.3390/RS6086929>
- Pongratz, J., Dolman, H., Don, A., Erb, K. H., Fuchs, R., Herold, M., et al. (2018). Models meet data: Challenges and opportunities in implementing land management in Earth system models. *Global Change Biology*, 24(4), 1470–1487. <https://doi.org/10.1111/GCB.13988>
- Reich, P. B., Hobbie, S. E., Lee, T. D., & Pastore, M. A. (2018). Unexpected reversal of C<sub>3</sub> versus C<sub>4</sub> grass response to elevated CO<sub>2</sub> during a 20-year field experiment. *Science*, 360(6386), 317–320. <https://doi.org/10.1126/SCIENCE.AAS9313>
- Sitch, S., Friedlingstein, P., Gruber, N., Jones, S. D., Murray-Tortarolo, G., Ahlström, A., et al. (2015). Recent trends and drivers of regional sources and sinks of carbon dioxide. *Biogeosciences*, 12(3), 653–679. <https://doi.org/10.5194/BG-12-653-2015>
- Smith, J., Lott, N., & Vose, R. (2011). The integrated surface database: Recent developments and partnerships. *Bulletin of the American Meteorological Society*, 92(6), 704–708. <https://doi.org/10.1175/2011BAMS3015.1>
- Smith, B., Wärlind, D., Arneth, A., Hickler, T., Leadley, P. W., Siltberg, J., & Zaehle, S. (2014). Implications of incorporating N cycling and N limitations on primary production in an individual-based dynamic vegetation model. *Biogeosciences*, 11(7), 2027–2054. <https://doi.org/10.5194/BG-11-2027-2014>
- Walker, A. P., Zaehle, S., Medlyn, B. E., Kauwe, M. G. D., Asao, S., Hickler, T., et al. (2015). Predicting long-term carbon sequestration in response to CO<sub>2</sub> enrichment: How and why do current ecosystem models differ? *Global Biogeochemical Cycles*, 29(4), 476–495. <https://doi.org/10.1002/2014GB004995>
- Wang, J. F., Li, X. H., Christakos, G., Liao, Y. L., Zhang, T., Gu, X., & Zheng, X. Y. (2010). Geographical detectors-based health risk assessment and its application in the neural tube defects study of the Heshun Region, China. *International Journal of Geographical Information Science*, 24(1), 107–127. <https://doi.org/10.1080/13658810802443457>
- Wang, X., Piao, S., Ciais, P., Li, J., Friedlingstein, P., Koven, C., & Chen, A. (2011). Spring temperature change and its implication in the change of vegetation growth in North America from 1982 to 2006. *Proceedings of the National Academy of Sciences of the United States of America*, 108(4), 1240–1245. <https://doi.org/10.1073/PNAS.1014425108>
- Wenzel, S., Cox, P. M., Eyring, V., & Friedlingstein, P. (2014). Emergent constraints on climate-carbon cycle feedbacks in the CMIP5 Earth system models. *Journal of Geophysical Research*, 119(5), 794–807. <https://doi.org/10.1002/2013JG002591>
- Wu, S., Gao, X., Lei, J., Zhou, N., & Wang, Y. (2020). Spatial and temporal changes in the normalized difference vegetation index and their driving factors in the desert/grassland biome transition zone of the Sahel region of Africa. *Remote Sensing*, 12(24), 4119. <https://doi.org/10.3390/rs12244119>
- Zeng, N., Zhao, F., Collatz, G. J., Kalnay, E., Salawitch, R. J., West, T. O., & Guanter, L. (2014). Agricultural Green Revolution as a driver of increasing atmospheric CO<sub>2</sub> seasonal amplitude. *Nature*, 515(7527), 394–397. <https://doi.org/10.1038/NATURE13893>
- Zhu, L., Meng, J., & Zhu, L. (2020). Applying Geodetector to disentangle the contributions of natural and anthropogenic factors to NDVI variations in the middle reaches of the Heihe River Basin. *Ecological Indicators*, 117, 106545. <https://doi.org/10.1016/j.ecolind.2020.106545>
- Zhu, Z., Piao, S., Myneni, R. B., Huang, M., Zeng, Z., Canadell, J. G., et al. (2016). Greening of the Earth and its drivers. *Nature Climate Change*, 6(8), 791–795. <https://doi.org/10.1038/NCLIMATE3004>